Eur. J. Stat. 4 (2024) 11
doi: 10.28924/ada/stat.4.11

Modeling and Prediction of Exchange Rates Using Topp-Leone Burr Type X, Machine Learning and Deep Learning Models

Hanita Daud[1], Aminu Suleiman Mohammed[2,*], Aliyu Ismail Ishaq[2], Badamasi Abba[3], Yahaya Zakari[2], Jamila Abdullahi[2], Dolapo Abidemi Shobanke[4], Ahmad Abubakar Suleiman[1]

[1]Fundamental and Applied Sciences Department, Universiti Teknologi PETRONAS, Seri Iskandar, 32610, Malaysia

Hanita_daud@utp.edu.my, Ahmad_22000579@utp.edu.my

[2]Department of Statistics, Ahmadu Bello University, Zaria, Nigeria

mohammedas@abu.edu.ng, binishaq05@gmail.com, yzakari@abu.edu.ng, jamilaa930@gmail.com

[3]School of Mathematics and Statistics, Central South University, Hunan, China

badamasiabba@gmail.com

[4]Department of Statistics, Federal University, Lokoja, Nigeria

dolapo.shobanke@fulokoja.edu.ng

Correspondence: aminusmohammed@gmail.com

ABSTRACT. This paper introduces the Topp-Leone Burr X distribution (TLBXD), a novel extension of the Burr X distribution, developed within the framework of the Topp-Leone-G family. The TLBXD is designed to effectively model varying datasets, addressing the limitations of classical distributions when applied to heterogeneous data. We derived and presented key mathematical and statistical properties of the TLBXD, ensuring their clarity and applicability for practical use. A simulation study was conducted to evaluate the efficiency of different parameter estimation methods, including least squares (LS), maximum product of spacings (MPS), weighted least squares (WLS), and maximum likelihood (ML). The proposed distribution was applied to two real-world dates related to the daily exchange rates of the Nigerian Naira against the EURO and RIYAL. The TLBXD demonstrated superior performance compared to existing sub-models. In addition to the data modeling, this research also applied the proposed distribution to explore the predictive capabilities of machine learning and deep learning techniques for exchange rate forecasting. Three machine learning models, including the Extreme Gradient Boosting (XGBoost), Random Forest, and Light Gradient Boosting Machine (LightGBM) were evaluated alongside a deep learning algorithm, the Long Short-Term Memory (LSTM). The models were trained on 80% of the data set and tested on the remaining 20% to assess prediction accuracy. The results reveal that the LSTM model has significantly outperformed the machine learning models in forecasting exchange rates, as evidenced by lower root means squared errors (RMSE) and mean absolute errors (MAE) values.

Received: 4 Sep 2024.

Key words and phrases. Burr X distribution; Topp-Leone distribution; Artificial intelligence; Machine learning; Exchange rate; Forecasting.

1. Introduction

An exchange rate is the price at which one currency can be swapped for another within a nation or economic zone. Because it is used to determine the relative values of other currencies, it is essential for understanding the dynamics of trade and capital flows. Two elements affect the rates: domestic currency value and foreign currency value. Exchange rates are subject to fluctuations due to many economic causes and variables. Exchange rates can change for several reasons, for example: Currency values and exchange rates are impacted by changes in interest rates. Assuming all other factors remain the same, a higher domestic interest rate will lead to a rise in the demand for domestic currency as more foreign investors will choose to invest at the higher interest rate, converting their foreign cash into local currency. However, inflationary forces counteract it. Another example is currency values and exchange rates, which are impacted by changes in inflation rates. When a local currency's value decreases over time more quickly than other foreign currencies, a greater inflation rate in that nation will, all other things being equal, reduce demand for that currency. Furthermore, the total amount of debt that the federal government has is known as its debt. It affects exchange rates and the value of currencies because a nation with more debt is less likely to attract foreign investment, which fuels inflation. It reduces the value of the local currency at exchange rates and exerts downward pressure on it. Consequently, [1] applied some probability models in forecasting the Southeast Asian currencies against the British Pound Sterling. Furthermore, [2] used another version of improved Dagun distribution to model financial datasets.

The addition of a shape parameter on Burr X plays an important role in terms of capturing the sensitive part of a given data thereby making the distribution possess heavy tails and a wide range of skewness. An attempt to fit diverse lifetime datasets to classical distributions has been very unsuccessful due to the heterogeneity of such datasets from assumed homogeneous populations.

Some of these data generated from different areas of study have been known to exhibit varying shapes, which makes it difficult for the known distributions to model. To cope with this, an improved or extended form of the existing or classical distributions is required, as compound distributions are found to be more robust when it comes to modelling data sets.

In the middle of the 20th century, [3] proposed different types of distribution functions for which Burr Type X distribution (BXD) was among. Bayesian estimation based on the

generalization of type-I hybrid censoring technique for Burr-X distribution by [4]. Another powerful extended version of Burr X was studied by [5], Using the Burr X distribution under the progressive-stress accelerated life test, several inferences based on progressively type-II censored data were examined by [6], The study examined revised test statistics for the double Burr type X distribution and its applications to right censored reliability and medical data by [7], also [8] proposed truncated Burr X-G class of distributions and also derived some of its desirable properties. The odd log-logistic Burr-x family of distributions which produced varieties of models was developed by [9], the Type I half logistic Burr X-G class by [10], and a robust Burr X-G class by [11]. In the year 2022, some inferences for stress–strength reliability of Burr X distribution based on ranked set sampling was carried out by [12], the statistics for BDX under progressively type-II censoring were studied by [13], and estimations were performed under Ranked Set Sampling for the Kavya–Manoharan–Burr X distribution by [14] and Gamma Odd Burr X-G Family was developed by [15] and Bayesian Inference analysis of the Unit–Power Burr type X model was investigated by [16].

The Topp-Leone distribution (TL), often known as the J-shaped distribution, is one of the continuous probability distributions used to represent lifespan datasets. This model was generated by [17] and has a closed form. Numerous authors developed some extensions of this distributions together with the exploration of its properties, for instant, [18] proposed Topp–Leone–G family distribution which has one parameter and capable of producing varying shapes, [19] explored and studied Power Topp–Leone distribution with its properties and applied the distribution on engineering data, a new version of the TL-class of models was studied by Muhammad *et al.* [20], an inference of multicomponent stress-strength reliability following TL distribution using progressively censored data was studied by [21], inference of Truncated Cauchy Power-Inverted TLdistribution under Hybrid Censored Scheme was carried out by [22], [23] proposed Topp-Leone type II exponentiated half logistic-G class which is capable of producing varying shapes, Alpha Power Topp-Leone Distribution by [24], a novel version of the Gamma-Topp-Leone-Type II-Exponentiated Half Logistic-G class by Oluyede and [25] and [26] studied the monotonic and non-monotonic hazard rates of Transmuted Exponential-Topp Leone distribution.

In essence, distributions are important when it comes to modeling and analyses of real-life data which led to the introduction of new distributions that are more robust when fitting data sets. However, the fitness of the assumed lifetime distribution is crucial to the quality

of any statistical analysis, which is one of the main driving forces for this work. The purpose of this research is to provide an alternative flexible distribution that can handle different skewed data sets that the current TL and Burr distributions are unable to adequately model. We are motivated by the need for robust and adaptable models in financial and lifetime data analysis, coupled with the growing importance of machine learning and deep learning in predictive modelling. The Topp-Leone-G family provides a flexible framework without introducing excessive complexity. The key achievements of the current investigation are as follows:

i. A novel flexible model, the TLBXD is developed, addressing the limitations of classical probability distributions in effectively modelling heterogeneous financial data.
ii. Describe a wide range of hazard rate patterns of the proposed distribution, thereby broadening its utility in risk analysis.
iii. employed machine learning and deep learning models including XGBoost, Random Forest, LightGBM, and LSTM, for comparative prediction of exchange rates, showcasing the TLBXD's potential in modern predictive analytics.
iv. Utilized the maximum likelihood estimation procedure for assessing the inferential features of the new distribution and to establish a comprehensive framework for practitioners in both statistical modelling and machine learning domains.
v. provided a workable distribution with applications in engineering, banking, and other fields for modelling asymmetric data, which is difficult for conventional distributions and prediction models to handle well.

The remainder of this paper is organized as follows: Section 2 focuses on the development of the TLBXD, including validity checks, graphical representations of the density and hazard functions, and an exploration of the statistical properties of the new TLBXD. Section 3 addresses the parameter estimation of the TLBXD, accompanied by simulation studies using various estimation methods, such as maximum likelihood estimation, least squares, maximum product of spacings, and weighted least squares. Section 4 discusses the application of the proposed TLBXD in the context of exchange rate prediction, particularly for the Nigerian Naira against the Euro and Riyal. Section 5 presents the application of machine learning and deep learning models, including XGBoost, Random Forest, LightGBM, and LSTM, to forecast exchange rate data, providing a comparative analysis of their performance. Finally, Section 6 concludes the paper by summarizing the

findings and potential implications of the proposed TLBXD and the predictive models used in this study.

2. Materials and Methods

2.1 Topp-Leone Burr Type X Distribution. Al-Shomrani *et al.* [18] proposed the distribution and probability density functions of the TL–G family which are respectively given as;

$$B(w;\alpha) = D(w)^{\alpha}\left(2 - D(w)\right)^{\alpha} \tag{1}$$

and,

$$b(w;\alpha) = 2\alpha d(w)\left(1 - D(w)\right)D(w)^{\alpha-1}\left(2 - D(w)\right)^{\alpha-1} \tag{2}$$

For, $w, \alpha > 0$

Now, consider the parent or baseline distribution to be Burr X with corresponding distribution and density functions which are respectively given as follows:

$$D(w) = \left(1 - e^{-w^2}\right)^{\theta} \tag{3}$$

and,

$$d(w) = 2\theta w e^{-w^2}\left(1 - e^{-w^2}\right)^{\theta-1} \tag{4}$$

By substituting equations (3) and (4) in (1) and (2), the Topp-Leone Burr type X distribution (TLBXD) was derived and has two shape parameters. The distribution and density functions are as follows:

$$B(w;\alpha,\theta) = \left(1 - e^{-w^2}\right)^{\theta\alpha}\left(2 - \left(1 - e^{-w^2}\right)^{\theta}\right)^{\alpha} \tag{5}$$

and,

$$b(w;\alpha,\theta) = 4\alpha\theta w e^{-w^2}\left(1 - e^{-w^2}\right)^{\theta-1}\left(1 - \left(1 - e^{-w^2}\right)^{\theta}\right)\left(1 - e^{-w^2}\right)^{\theta(\alpha-1)}\left(2 - \left(1 - e^{-w^2}\right)^{\theta}\right)^{\alpha-1} \tag{6}$$

For, $w, \alpha, \theta > 0$.

Equation (6) can be reduced as

$$b(w;\alpha,\theta) = 4\alpha\theta w e^{-w^2}\left(1 - e^{-w^2}\right)^{\theta\alpha-1}\left(1 - \left(1 - e^{-w^2}\right)^{\theta}\right)\left(2 - \left(1 - e^{-w^2}\right)^{\theta}\right)^{\alpha-1}$$

Fact 1: The pdf of a continuous random variable that follows TLBXD is equal to one.

$$\int_0^{\infty} b(w;\alpha,\theta)dw = 1$$

Proof:

$$\int_0^{\infty} 4\alpha\theta w e^{-w^2}\left(1-e^{-w^2}\right)^{\theta-1}\left(1-\left(1-e^{-w^2}\right)^{\theta}\right)\left(1-e^{-w^2}\right)^{\theta(\alpha-1)}\left(2-\left(1-e^{-w^2}\right)^{\theta}\right)^{\alpha-1} dw$$

$$\text{Let, } u=\left(1-e^{-w^2}\right)^{\theta}, as\ w\to 0, u\to 0 \& w\to\infty, u\to 1,$$

$$dw=\frac{du}{2\theta w e^{-w^2}\left(1-e^{-w^2}\right)^{\theta-1}}$$

$$\int_0^{1} 4\alpha\theta w e^{-w^2}\left(1-e^{-w^2}\right)^{\theta-1}(1-u)u^{(\alpha-1)}(2-u)^{\alpha-1}\frac{du}{2\theta w e^{-w^2}\left(1-e^{-w^2}\right)^{\theta-1}}$$

$$\int_0^{1} 2\alpha(1-u)\left(u(2-u)\right)^{\alpha-1} du$$

$$\text{Let, } z=u(2-u)=2u-u^2, du=\frac{dz}{2(1-u)}$$

$$\int_0^{1} 2\alpha(1-u)z^{\alpha-1}\frac{dz}{2(1-u)}$$

$$\int_0^{1} \alpha z^{\alpha-1}dz=\alpha\left[\frac{z^{\alpha}}{\alpha}\right]_0^1=1.$$

Indeed, the TLBXD is a proper distribution.

2.2 Graphical Representation of the TLBXD's Density and Distribution Functions. Fig. 1 and 2 respectively exhibit the plots of the pdf and distribution function for a few chosen parameter values.

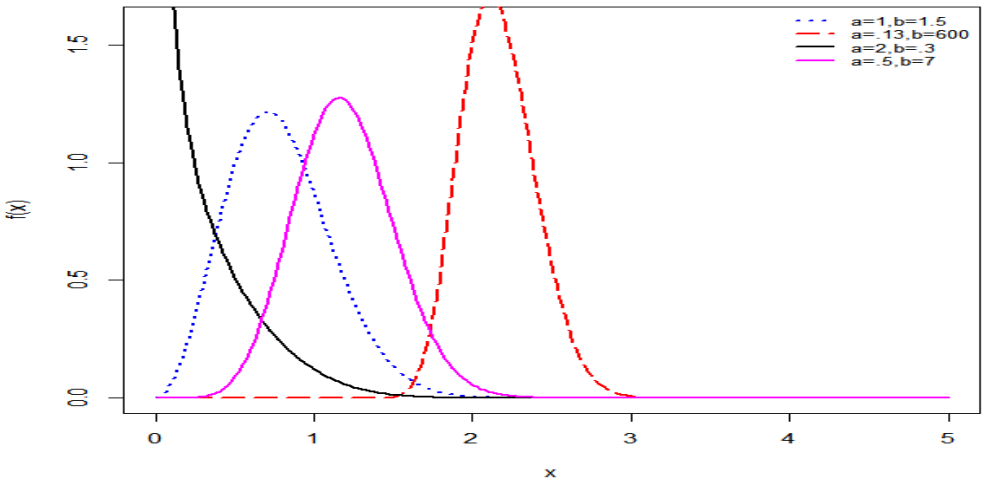

Figure 1. Plot of the pdf for TLBXD

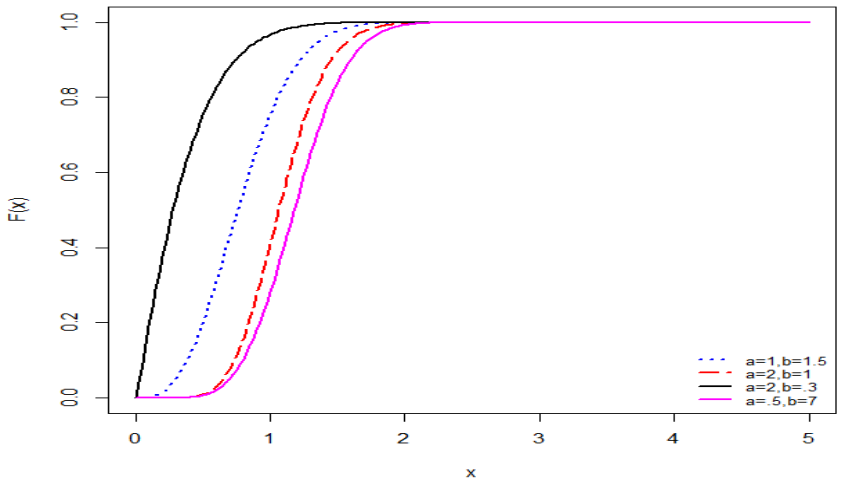

Figure 2. The plot of the distribution function for TLBXD

2.3 Statistical properties of TLBXD. Here, some basic features of TLBXD are provided in an explicit form.

2.3.1 Asymptotic Behavior of the Distribution Function of the TLBXD. Here, the asymptotic behavior of the TLBXD is examined by considering the limit $as\, w \to 0 \, and \, w \to \infty$ of the density and distribution function.

$$\lim_{w\to 0} B(w;\alpha,\theta) = \lim_{w\to 0}\left(1-e^{-w^2}\right)^{\theta\alpha}\left(2-\left(1-e^{-w^2}\right)^{\theta}\right)^{\alpha} = 0$$

and,

$$\lim_{w\to \infty} B(w;\alpha,\theta) = \lim_{w\to \infty}\left(1-e^{-w^2}\right)^{\theta\alpha}\left(2-\left(1-e^{-w^2}\right)^{\theta}\right)^{\alpha} = 1$$

These results further prove that the TLBXD is a proper (valid) distribution.

2.3.2 Survival and Hazard Functions of TLBXD. The explicit definitions of the survival and hazard functions are, respectively, derived as follows:

$$S(w;\alpha,\theta) = 1-\left(1-e^{-w^2}\right)^{\theta\alpha}\left(2-\left(1-e^{-w^2}\right)^{\theta}\right)^{\alpha} \tag{7}$$

and

$$h(w;\alpha,\theta) = \frac{4\alpha\theta w e^{-w^2}\left(1-e^{-w^2}\right)^{\theta-1}\left(1-\left(1-e^{-w^2}\right)^{\theta}\right)\left(1-e^{-w^2}\right)^{\theta(\alpha-1)}\left(2-\left(1-e^{-w^2}\right)^{\theta}\right)^{\alpha-1}}{1-\left[\left(1-e^{-w^2}\right)^{\theta\alpha}\left(2-\left(1-e^{-w^2}\right)^{\theta}\right)^{\alpha}\right]} \tag{8}$$

Fig. 3 and 4 show the plots of the survival and hazard functions for a few chosen values of parameters.

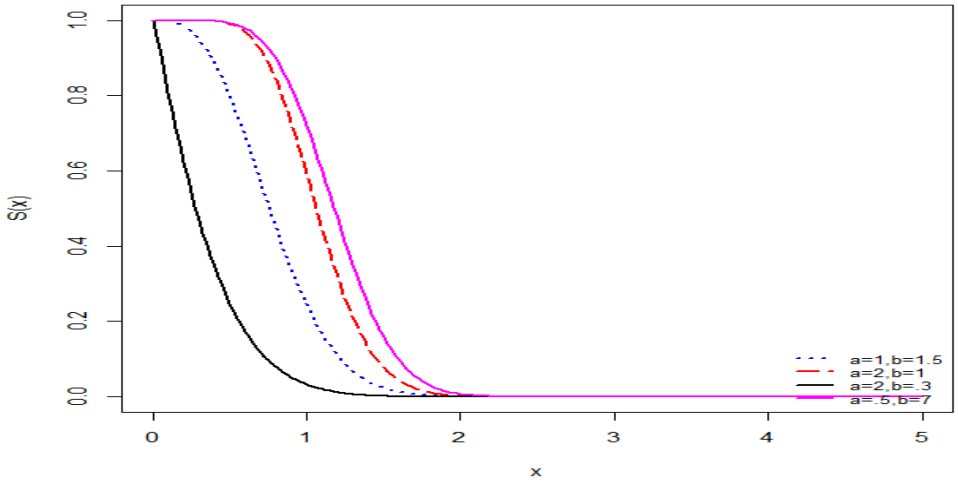

Figure 3. Plot of the survival function of the TLBXD

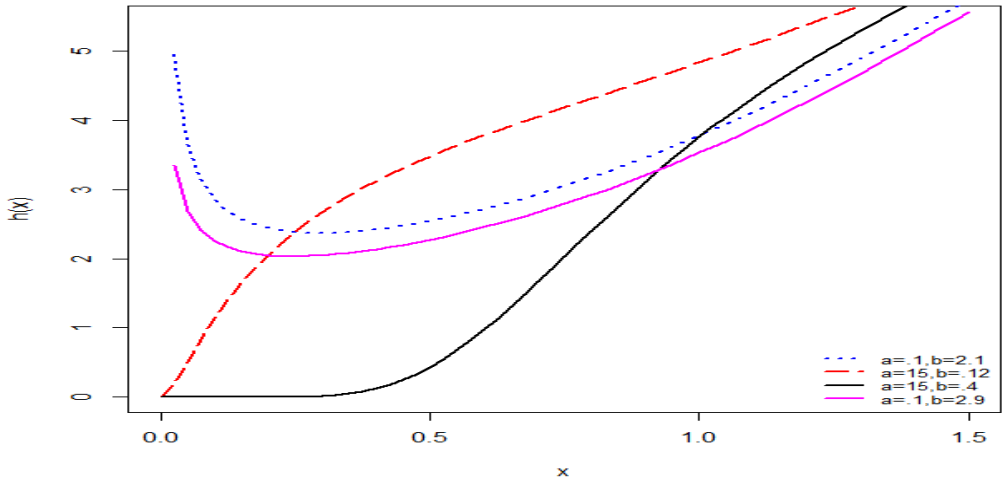

Figure 4. Plot of the hazard function of the TLBXD

Series expansion of the TLBXD

The density function in equation (6) can be rewritten as;

$$b(w;\alpha,\theta)=4\alpha\theta we^{-w^2}\left(1-e^{-w^2}\right)^{\theta-1}\left(1-\left(1-e^{-w^2}\right)^{\theta}\right)\left[1-\left(1-\left(1-e^{-w^2}\right)^{\theta}\right)^{2}\right]^{\alpha-1}$$

Recall that,

$$(1-K)^{b-1}=\sum_{j=0}^{\infty}(-1)^{j}\binom{b-1}{j}K^{j}$$

So,

$$\left[1-\left(1-\left(1-e^{-w^2}\right)^{\theta}\right)^2\right]^{\alpha-1}=\sum_{a=0}^{\infty}(-1)^a\binom{\alpha-1}{a}\left(1-\left(1-e^{-w^2}\right)^{\theta}\right)^{2a}$$

$$b(w;\alpha,\theta)=4\alpha\theta we^{-w^2}\left(1-e^{-w^2}\right)^{\theta-1}\sum_{a=0}^{\infty}(-1)^a\binom{\alpha-1}{a}\left(1-\left(1-e^{-w^2}\right)^{\theta}\right)^{2a+1}$$

again, $$\left(1-\left(1-e^{-w^2}\right)^{\theta}\right)^{2a+1}=\sum_{b=0}^{\infty}(-1)^b\binom{2a+1}{b}\left(1-e^{-w^2}\right)^{\theta b}$$

$$b(w;\alpha,\theta)=4\alpha\theta we^{-w^2}\sum_{a,b=0}^{\infty}(-1)^{a+b}\binom{\alpha-1}{a}\binom{2a+1}{b}\left(1-e^{-w^2}\right)^{\theta(1+b)-1}$$

but $$\left(1-e^{-w^2}\right)^{\theta(1+b)-1}=\sum_{c=0}^{\infty}(-1)^c\binom{\theta(1+b)-1}{c}e^{-cw^2}$$

$$b(w;\alpha,\theta)=4\alpha\theta\sum_{a,b,c=0}^{\infty}(-1)^{a+b+c}\binom{\alpha-1}{a}\binom{2a+1}{b}\binom{\theta(1+b)-1}{c}we^{-(1+c)w^2}$$

$$b(w;\alpha,\theta)=4\alpha\theta M_{a,b,c}\,we^{-(1+c)w^2} \tag{9}$$

where, $$M_{a,b,c}=\sum_{a,b,c=0}^{\infty}(-1)^{a+b+c}\binom{\alpha-1}{a}\binom{2a+1}{b}\binom{\theta(1+b)-1}{c}$$

2.3.3 Moment and Moment Generating Functions of TLBXD. Proposition 1: The r[th] moment of TLBXD is provided by;

$$\mu_r^{'}=\frac{2\alpha\theta M_{a,b,c}\left|\left(\frac{r}{2}+1\right)\right.}{(1+c)^{\frac{r}{2}+1}} \tag{10}$$

Where, $M_{a,b,c}=\sum_{a,b,c=0}^{\infty}(-1)^{a+b+c}\binom{\alpha-1}{a}\binom{2a+1}{b}\binom{\theta(1+b)-1}{c}$

Proof:

$$\mu_r^{'}=E(w^r)=\int_0^{\infty}w^r b(w;\alpha,\theta)dw$$

$$\mu_r^{'}=\int_0^{\infty}w^r\,4\alpha\theta M_{a,b,c}\,we^{-(1+c)w^2}dw$$

$$=4\alpha\theta M_{a,b,c}\int_0^{\infty}w^{r+1}e^{-(1+c)w^2}dw$$

Let, $y=(1+c)w^2$, $w=\frac{y^{\frac{1}{2}}}{(1+c)^{\frac{1}{2}}}$, $dw=\frac{\frac{1}{2}y^{-\frac{1}{2}}}{(1+c)^{\frac{1}{2}}}dy$

$$= 4\alpha\theta M_{a,b,c}\int_0^{\infty}\left(\frac{y}{1+c}\right)^{\frac{1}{2}(r+1)} e^{-y}\frac{\frac{1}{2}y^{-\frac{1}{2}}}{(1+c)^{\frac{1}{2}}}dy$$

$$= \frac{2\alpha\theta M_{a,b,c}}{(1+c)^{\frac{r}{2}+1}}\int_0^{\infty} y^{(\frac{r}{2}+1)-1}e^{-y}dy = \frac{2\alpha\theta M_{a,b,c}}{(1+c)^{\frac{r}{2}+1}}\left|\left(\frac{r}{2}+1\right)\right.$$

The Moment Generating function (MGF)

Proposition 2: The MGF is given by;

$$M_W(t) = \sum_{d=0}^{\infty}\frac{2\alpha\theta t^d M_{abc}}{d!(1+c)^{\frac{d}{2}+1}}\left|\left(\frac{d}{2}+1\right)\right. \tag{11}$$

where, $M_{a,b,c} = \sum_{a,b,c=0}^{\infty}(-1)^{a+b+c}\binom{\alpha-1}{a}\binom{2a+1}{b}\binom{\theta(1+b)-1}{c}$

Proof:

$$M_W(t) = E(e^{tw}) = \int_0^{\infty} e^{tw}b(w;\alpha,\theta)dw$$

$$e^{tw} = \sum_{d=0}^{\infty}\frac{t^d w^d}{d!}$$

$$M_W(t) = \sum_{d=0}^{\infty}\frac{t^d}{d!}\int_0^{\infty} w^d b(w;\alpha,\theta)dw = \sum_{d=0}^{\infty}\frac{t^d}{d!}\mu_d^{'}$$

$$M_W(t) = \sum_{d=0}^{\infty}\frac{2\alpha\theta t^d M_{abc}}{d!(1+c)^{\frac{d}{2}+1}}\left|\left(\frac{d}{2}+1\right)\right.$$

2.3.4 Quantile Function of TLBXD. Proposition 3: The quantile function (qf) of the proposed model is simplified as;

$$w_u = \left(-\ln\left(1-\left(1-\sqrt{1-u^{\frac{1}{\alpha}}}\right)^{\frac{1}{\theta}}\right)\right)^{\frac{1}{2}} \tag{12}$$

Proof:

Recall that, the of the Topp-Leone-G is given as;

$$Q_{TL-G} = D^{-1}\left(1-\sqrt{1-u^{\frac{1}{\alpha}}}\right),$$

Also,

$$D(w;\alpha,\theta)=\left(1-e^{-w^2}\right)^{\theta}$$

$$u=\left(1-e^{-w^2}\right)^{\theta}$$

$$u^{\frac{1}{\theta}}=\left(1-e^{-w^2}\right)$$

$$e^{-w^2}=1-u^{\frac{1}{\theta}}$$

$$w^2=-\ln\left(1-u^{\frac{1}{\theta}}\right)$$

but,

$$u=\left(1-\sqrt{1-u^{\frac{1}{\alpha}}}\right)$$

$$w_u=\left(-\ln\left(1-\left(1-\sqrt{1-u^{\frac{1}{\alpha}}}\right)^{\frac{1}{\theta}}\right)\right)^{\frac{1}{2}}$$

Table 1. Some chosen measures of $W\sim TLBXD$ for some selected values of the parameters $\alpha=0.5 and\ \theta=0.5, 1, 1.5, 2 \& 2.5$.

	0.5	1.0	1.5	2.0	2.5
Mean	0.2373	0.4469	0.5966	0.709	0.7976
Variance	0.0773	0.1134	0.1234	0.1245	0.1224
Skewness	1.7107	0.9887	0.7124	0.5714	0.4895
Kurtosis	6.2100	3.7905	3.2851	3.1281	3.0737

Table 2. Some chosen measures of $W \sim TLBXD$ for some selected values of the parameters $\theta = 0.5 \, and \; \alpha = 0.5, 1, 1.5, 2 \& 2.5$.

	0.5	1.0	1.5	2.0	2.5
Mean	0.2373	0.3733	0.4663	0.5358	0.5906
Variance	0.0773	0.0940	0.0977	0.0975	0.0960
Skewness	1.7107	1.2002	0.9948	0.8875	0.8239
Kurtosis	6.2100	4.4663	3.9939	3.8082	3.7224

From Table 1, we can see that as the value of the parameter "theta" rises and for a fixed value of "alpha", the mean also increases while skewness and kurtosis decrease as the parameter "theta" increases. Furthermore, the variance decreases to some certain point and increases as the value of "theta" gets large. Consequently, from Table 2, as the value of the parameter "theta" increases and for a fixed value of "alpha", the mean also increases while skewness and kurtosis reduce as the parameter "theta" increases. Furthermore, the variance reduces to some certain point and increases as the value of "theta" gets large.

2.3.5 Power Weighted Moments of the TLBX Distribution

$$P_{r,q} = \int_{-\infty}^{\infty} w^r f(w) F(w)^q dw \tag{13}$$

Where $F(w)$ and $f(w)$ are the cdf and pdf of any continuous distribution respectively. Now, substituting the cdf and pdf of TLBXD in (13) gives,

$$P_{r,q} = 4\alpha\theta \int_0^{\infty} w^{r+1} e^{-w^2} \left(1-e^{-w^2}\right)^{\theta\alpha-1} \left(1-\left(1-e^{-w^2}\right)^{\theta}\right) \left(2-\left(1-e^{-w^2}\right)^{\theta}\right)^{\alpha-1}$$

$$\left\{\left(1-e^{-w^2}\right)^{\theta\alpha} \left(2-\left(1-e^{-w^2}\right)^{\theta}\right)^{\alpha}\right\}^{q} dw$$

$$= 4\alpha\theta \int_0^{\infty} w^{r+1} e^{-w^2} \left(1-e^{-w^2}\right)^{\theta\alpha(1+q)-1} \left(1-\left(1-e^{-w^2}\right)^{\theta}\right) \left(2-\left(1-e^{-w^2}\right)^{\theta}\right)^{\alpha(1+q)-1} dw$$

$$P_{r,q} = 4\alpha\theta \int_0^{\infty} w^{r+1} e^{-w^2} \left(1-e^{-w^2}\right)^{\theta\alpha(1+q)-1} \left(1-\left(1-e^{-w^2}\right)^{\theta}\right) \left(1+\left\{1-\left(1-e^{-w^2}\right)^{\theta}\right\}\right)^{\alpha(1+q)-1} dw \tag{14}$$

Consider the binomial expansion given as

$$(1+x)^n = \sum_{i=0}^{n} \binom{n}{i} x^i \tag{15}$$

Applying (15) into (14), it becomes

$$P_{r,q} = 4\alpha\theta \int_0^\infty w^{r+1} e^{-w^2} \left(1-e^{-w^2}\right)^{\theta\alpha(1+q)-1} \left(1-\left(1-e^{-w^2}\right)^{\theta}\right) \sum_{i=0}^{n} \binom{\alpha(1+q)-1}{i} \left\{1-\left(1-e^{-w^2}\right)^{\theta}\right\}^i dw$$

$$P_{r,q} = 4\alpha\theta \int_0^\infty w^{r+1} e^{-w^2} \left(1-e^{-w^2}\right)^{\theta\alpha(1+q)-1} \sum_{i=0}^{n} \binom{\alpha(1+q)-1}{i} \left\{1-\left(1-e^{-w^2}\right)^{\theta}\right\}^{i+1} dw \tag{16}$$

Let us consider the expansion

$$(1-x)^n = \sum_{j=0}^{n} (-1)^j \binom{n}{j} x^j \tag{17}$$

Substituting (5) into (4), we have,

$$P_{r,q} = 4\alpha\theta \int_0^\infty w^{r+1} e^{-w^2} \left(1-e^{-w^2}\right)^{\theta\alpha(1+q)-1} \sum_{i=0}^{n} \binom{\alpha(1+q)-1}{i} \sum_{j=0}^{n} (-1)^j \binom{i+1}{j} \left(1-e^{-w^2}\right)^{\theta j} dw$$

$$= 4\alpha\theta \int_0^\infty w^{r+1} e^{-w^2} \left(1-e^{-w^2}\right)^{\theta\alpha(1+q)-1} \sum_{i,j=0}^{n} (-1)^j \binom{\alpha(1+q)-1}{i} \binom{i+1}{j} \left(1-e^{-w^2}\right)^{\theta j} dw$$

$$P_{r,q} = 4\alpha\theta \sum_{i,j=0}^{n} \Omega_{i,j} \int_0^\infty w^{r+1} e^{-w^2} \left(1-e^{-w^2}\right)^{\theta[\alpha(1+q)+j]-1} dw$$

Where $\Omega_{i,j} = (-1)^j \binom{\alpha(1+q)-1}{i} \binom{i+1}{j}$

$$= 4\alpha\theta \sum_{i,j=0}^{n} \Omega_{i,j} \int_0^\infty w^{r+1} e^{-w^2} \sum_{k=0}^{n} (-1)^k \binom{\theta[\alpha(1+q)+j]-1}{k} e^{-kw^2} dw$$

$$P_{r,q} = 4\alpha\theta \sum_{i,j,k=0}^{n} Z_{i,j,k} \int_0^\infty w^{r+1} e^{-(1+k)w^2} dw$$

where,

$$Z_{i,j,k} = \Omega_{i,j} (-1)^k \binom{\theta[\alpha(1+q)+j]-1}{k}$$

Now let,

$$m = (1+k)w^2; \; dw = \frac{dm}{2(1+k)w}$$

$$P_{r,q} = 4\alpha\theta \sum_{i,j,k=0}^{n} Z_{i,j,k} \int_0^\infty w^{r+1} e^{-m} \frac{dm}{2(1+k)w}$$

$$= 2\alpha\theta \sum_{i,j,k=0}^{n} Z_{i,j,k} \frac{1}{(1+k)} \int_0^{\infty} \left(\frac{m}{1+k}\right)^{\frac{r}{2}} e^{-m} dm$$

$$P_{r,q} = \frac{2\alpha\theta}{(1+k)^{\frac{r}{2}+1}} \sum_{i,j,k=0}^{n} Z_{i,j,k} \left|\left(\frac{r}{2}+1\right)\right. \tag{18}$$

$$\text{where, } Z_{i,j,k} = \Omega_{i,j}(-1)^k \binom{\theta[\alpha(1+q)+j]-1}{k}$$

Which is the PWM of the TLBX distribution.

2.3.5 Maximum Likelihood Estimation (MLE) of TLBXD. The estimation of the unknown parameters of TLBXD is as follows:

Let, $w_1, w_2, ..., w_n$ be a random sample (r.s) of size n from the from the TLBXD, then the log-likelihood of the density function is derived as:

$$L = n\log 4 + n\log\alpha + n\log\theta + \sum_{i=1}^{n}\log w_i - \sum_{i=1}^{n} w_i^2 + (\theta\alpha - 1)\sum_{i=1}^{n}\log\left(1-e^{-w_i^2}\right) + \sum_{i=1}^{n}\left(1-\left(1-e^{-w_i^2}\right)^{\theta}\right) + (\alpha-1)\sum_{i=1}^{n}\log\left(2-\left(1-e^{-w_i^2}\right)^{\theta}\right) \tag{19}$$

$$\frac{\delta L}{\delta\alpha} = \frac{n}{\alpha} + \theta\sum_{i=1}^{n}\log\left(1-e^{-w_i^2}\right) + \sum_{i=1}^{n}\log\left(2-\left(1-e^{-w_i^2}\right)^{\theta}\right) \tag{20}$$

$$\frac{\delta L}{\delta\alpha} = \frac{n}{\theta} + \alpha\sum_{i=1}^{n}\log\left(1-e^{-w_i^2}\right) - \sum_{i=1}^{n}\frac{\left(1-e^{-w_i^2}\right)^{\theta}\ln\left(1-e^{-w_i^2}\right)}{\left(1-\left(1-e^{-w_i^2}\right)^{\theta}\right)} - (\alpha-1)\sum_{i=1}^{n}\frac{\left(1-e^{-w_i^2}\right)^{\theta}\ln\left(1-e^{-w_i^2}\right)}{\left(2-\left(1-e^{-w_i^2}\right)^{\theta}\right)} \tag{21}$$

The ML Estimator of the parameters is derived by setting the equations (20 and 21) to zero. The solutions will give the corresponding estimators of the parameters. From the look of the equations, an optimization technique needs to be employed to numerically maximize the log-like likelihood function.

3. Estimation of Parameter

Here, we discussed and presented different estimation approaches to estimate the TLBX parameters, viz.: least-square (LS), maximum product of spacings (MPS), weighted least-square (WLS), maximum likelihood (ML) methods. Here, the effectiveness of the estimation processes in estimating the TLBXD parameters is assessed by Monte Carlo simulation experiments. The steps of the simulation algorithm are explained as follows:

i. set the sample size n and initialize the values of the parameters, α and θ

ii. to generate a random sample of size n from the TLBX distribution, use the quantile function of the TLBXD

iii. compute the model's parameter estimates

iv. steps (ii) and (iii) should be repeated N times.

The R software was used to run the simulation, and N = 1000 Monte Carlo replications were used. We consider n=25, 50, 100, 200, 300, and 500, together with fixed model parameter values.

From Tables 3 and 4, the methods that were employed in the estimation of the TLBXD's parameters provide more efficient and consistent results as the sample size rises. The estimates tend to move closer to the actual value as parameter as we have in Tables 3 and 4 as the size increases. Furthermore, the MSEs, Biases decreases with an increase in sample size.

Table 3: Means, Biases, and MSEs for the different estimation procedures

n	Parameter	LSE			MPS		
		Mean	Bias	MSE	Mean	Bias	MSE
25	α=1	1.137	0.137	0.705	1.2135	0.2135	2.2629
	θ=1.5	1.9888	0.4888	1.738	2.5263	1.0263	4.2684
50	α=1	1.1075	0.1075	0.514	1.1002	0.1002	1.0145
	θ=1.5	1.8201	0.3201	0.908	2.1508	0.6508	2.137
100	α=1	1.0826	0.0826	0.353	1.0256	0.0256	0.4744
	θ=1.5	1.7088	0.2088	0.521	1.8758	0.3758	0.9173
200	α=1	1.0593	0.0593	0.228	0.9954	-0.005	0.2257
	θ=1.5	1.628	0.128	0.292	1.7139	0.2139	0.3768
300	α=1	1.055	0.055	0.166	0.9994	-6E-04	0.1659
	θ=1.5	1.5845	0.0845	0.2	1.6454	0.1454	0.2259
500	α=1	1.0331	0.0331	0.105	0.9897	-0.01	0.0879
	θ=1.5	1.5602	0.0602	0.131	1.5967	0.0967	0.1278

Table 4: Means, Biases, and MSEs for the different estimation procedures

N	Parameter	WLSE			MLE		
		Mean	Bias	MSE	Mean	Bias	MSE
25	α=1	1.178	0.178	0.8825	1.3639	0.3639	0.4831
	θ=1.5	2.0453	0.5453	2.0813	1.4031	-0.097	0.2421
50	α=1	1.2088	0.2088	0.7644	1.2818	0.2818	0.3851
	θ=1.5	1.799	0.299	1.0249	1.4381	-0.062	0.2104
100	α=1	1.1484	0.1484	0.4453	1.1959	0.1959	0.2964
	θ=1.5	1.6656	0.1656	0.5296	1.479	-0.021	0.1831
200	α=1	1.1053	0.1053	0.2709	1.137	0.137	0.2099
	θ=1.5	1.5862	0.0862	0.2733	1.4979	-0.002	0.1508
300	α=1	1.0759	0.0759	0.1738	1.1135	0.1135	0.1602
	θ=1.5	1.5589	0.0589	0.1875	1.4921	-0.008	0.1177
500	α=1	1.045	0.045	0.1064	1.0795	0.0795	0.106
	θ=1.5	1.5427	0.0427	0.1179	1.4943	-0.006	0.0872

Table 5: Summary for the MSEs of the various methods of estimations

n	Parameter	LSE	MPS	WLSE	MLE
25	α=1	0.705	2.2629	0.8825	0.4831
	θ=2.5	1.738	4.2684	2.0813	0.2421
50	α=1	0.514	1.0145	0.7644	0.3851
	θ=2.5	0.908	2.137	1.0249	0.2104
100	α=1	0.353	0.4744	0.4453	0.2964
	θ=2.5	0.521	0.9173	0.5296	0.1831
200	α=1	0.228	0.2257	0.2709	0.2099
	θ=2.5	0.292	0.3768	0.2733	0.1508
300	$\alpha = 1$	0.166	0.1659	0.1738	0.1602
	$\theta = 2.5$	0.2	0.2259	0.1875	0.1177
500	$\alpha = 1$	0.105	0.0879	0.1064	0.106
	$\theta = 2.5$	0.131	0.1278	0.1179	0.0872

Based on the summary results for the MSE in table 5, the MLE has the least value and as such outperformed all the methods considered in this study.

From Tables 6 and 7, the methods that were employed in the estimation of the TLBXD's parameters provide more efficient and consistent results as the sample size rises. The estimates tend to move closer to the actual value as parameter as we have in Tables 6 and

7 as the size increases. Furthermore, the MSEs, Biases decreases with an increase in sample size.

Table 6: Means, Biases, and MSEs for the LSE and MPS estimation procedures

n	Parameter	LSE			MPS		
		Mean	Bias	MSE	Mean	Bias	MSE
25	α=1	1.1117	0.1117	0.5838	1.1386	0.1386	1.5149
	θ=2.5	3.1707	0.6707	3.4695	4.0859	1.5859	10.3551
50	α=1	1.0891	0.0891	0.4329	1.0648	0.0648	0.7917
	θ=2.5	2.9700	0.4700	2.0826	3.4527	0.9527	4.6674
100	α=1	1.0686	0.0686	0.2928	1.0303	0.0303	0.4756
	θ=2.5	2.7990	0.2990	1.1853	3.0886	0.5886	2.2966
200	α=1	1.0524	0.0524	0.1981	0.9970	-0.003	0.2161
	θ=2.5	2.6941	0.1941	0.7222	2.8354	0.3354	0.9575
300	α=1	1.0510	0.0510	0.1481	0.9942	-0.006	0.1505
	θ=2.5	2.6288	0.1288	0.5080	2.7434	0.2434	0.6212
500	α=1	1.0358	0.0358	0.1033	0.9870	-0.013	0.0818
	θ=2.5	2.5933	0.0933	0.3537	2.6606	0.1606	0.3450

Table 7: Means, Biases, and MSEs for the WLSE and MLE estimation procedures

N	Parameter	WLSE			MLE		
		Mean	Bias	MSE	Mean	Bias	MSE
25	α=1	1.1446	0.1446	0.7428	1.3985	0.3985	0.4692
	θ=2.5	3.2576	0.7576	4.2382	2.2267	-.2733	0.5239
50	α=1	1.1426	0.1426	0.5398	1.3133	0.3133	0.3701
	θ=2.5	2.9539	0.4539	2.3056	2.293	-.207	0.4459
100	α=1	1.1232	0.1232	0.3588	1.2259	0.2259	0.2817
	θ=2.5	2.7544	0.2544	1.3119	2.3661	-.1339	0.378
200	α=1	1.0839	0.0839	0.2088	1.1633	0.1633	0.1967
	θ=2.5	2.6377	0.1377	0.6943	2.4094	-.0906	0.3044
300	$\alpha = 1$	1.0756	0.0756	0.1632	1.1322	0.1322	0.1508
	$\theta = 2.5$	2.5886	0.0886	0.4950	2.425	-.075	0.2463
500	$\alpha = 1$	1.0491	0.0491	0.0997	1.0918	0.0918	0.0998
	$\theta = 2.5$	2.5582	0.0582	0.3163	2.4501	-.0499	0.19

Table 8: Summary for the MSEs of the various methods of estimations

n	Parameter	LSE	MPS	WLSE	MLE
25	α=1	0.5838	1.5149	0.7428	0.4692
	θ=2.5	3.4695	10.3551	4.2382	0.5239
50	α=1	0.4329	0.7917	0.5398	0.3701
	θ=2.5	2.0826	4.6674	2.3056	0.4459
100	α=1	0.2928	0.4756	0.3588	0.2817
	θ=2.5	1.1853	2.2966	1.3119	0.378
200	α=1	0.1981	0.2161	0.2088	0.1967
	θ=2.5	0.7222	0.9575	0.6943	0.3044
300	$\alpha = 1$	0.1481	0.1505	0.1632	0.1508
	$\theta = 2.5$	0.5080	0.6212	0.4950	0.2463
500	$\alpha = 1$	0.1033	0.0818	0.0997	0.0998
	$\theta = 2.5$	0.3537	0.3450	0.3163	0.19

Based on the summary results for the MSE in table 8, the MLE has the least value and as such outperformed all the methods considered in this study.

From Tables 3 and 4, the methods that were employed in the estimation of the TLBXD's parameters provide more efficient and consistent results as the sample size increases. The estimates tend to approach the actual value as parameter as we have in Tables 3 and 4 as "n" increases. Furthermore, the MSEs, Biases reduces with an increase in sample size.

4. Exchange Rates Prediction Using Proposed TLBXD

In this study, two data sets are utilized to compare the performance of the generated Topp Leone-Burr X model against other existing distributions, specifically the Burr X, Topp Leone, and Marshall-Olkin-Burr X distributions. The data sets represent the daily Nigerian exchange rate between the Euro and Saudi Riyal for the period from January 3rd, 2023, to December 29th, 2023, and can be obtained at

https://www.cbn.gov.ng/rates/ExchRateByCurrency.asp.

Due to the Topp-Leone model's range intervals, the data sets were transformed using the Topp-Leone's limitations, multiplying the observations by a constant k so that $k=5\times10^{-4}$. The goodness-of-fit measures for the Nigerian Naira to Saudi Riyal exchange rates data are presented in Tables 9 and 10.

Table 9: Goodness-of-fit measures for the Nigerian Naira to Saudi Riyal exchange rates data

Model	Estimate	BIC	AIC	CAIC	HQIC	LL
TL-BX	$a=1092.0000$	-584.4836	-591.4532	-591.4028	-588.6453	297.7266
	$\theta=0.0061$					
TL	$a=0.5425$	-396.8964	-400.3812	-400.3645	-398.9772	201.1906
BX	$\theta=0.2004$	-271.4084	-274.8932	-274.8765	-273.4892	138.4466
MO-BX	$k=0.0002$	-566.0308	-573.0004	-572.9500	-570.1925	288.5002
	$\theta=2.2120$					

Table 10: Goodness-of-fit measures for the monthly Nigerian Naira to Euro exchange rates data

Model	Estimate	BIC	AIC	CAIC	HQIC	LL
TL-BX	$a=2618.0000$	-236.2518	-243.2214	-243.1710	-240.4135	123.6107
	$\theta=0.0086$					
TL	$a=1.6976$	-173.0963	-176.5811	-176.5644	-175.1771	89.2906
BX	$\theta=0.4461$	49.8419	46.3571	46.3738	47.7610	-22.1785
MO-BX	$k=20.0100$	485.5760	478.6064	478.6568	481.4143	-237.3032
	$\theta=0.1000$					

As shown in Tables 9 and 10, the suggested Topp Leone-Burr X distribution produced the lowest values for the BIC, AIC, HQIC, and HQIC with relation to the alternative comparators, resulting in the highest values for the LL. This demonstrates that the new distribution can be chosen as the optimal distribution for both data sets.

5. Exchange Rates Prediction Using Machine Learning (ML) and Deep Learning (DL) Models

The daily exchange rates of the Nigerian Naira against the EURO and RIYAL from January 2020 to December 2023 were analyzed in the previous section using probability distributions. The objective was to compare the suggested distribution with other well-known distributions from statistical literature, aiming to demonstrate the potential applicability of the proposed TLBXD as a reliable lifetime model. In this section, we examine three machine learning models and a deep learning algorithm in a comparative analysis, assessing their prediction abilities using the same datasets. Extreme Gradient Boosting (XGBoost), Random Forest,

and Light Gradient Boosting Machine (LightGBM) are the machine learning models under consideration. In contrast, the Long Short-Term Memory (LSTM) represents the deep learning algorithm. The primary objective is to assess the accuracy of exchange rate forecasts for both ML and DL techniques. In order to enable efficient model fitting, 80% of the data has been set up for training, and the remaining 20% is retained for testing in order to assess prediction accuracy.

Figure 5 shows the line graph of the Nigerian Naira's exchange rates against the EURO and RIYAL for the period of January 2020 to December 2023 showed an apparent and consistent increasing trend. That means that there was an obvious rise in these currency values from June 2023 to December 2023. This sudden increase in currency rates highlights the Naira's alarming decrease against the EURO and RIYAL. The depicted line graphs not only serve as a visual representation of the currency fluctuations but also emphasize the severity of the Naira's devaluation during the latter half of 2023. This decline is particularly alarming, emphasizing the economic challenges faced by Nigeria in maintaining a stable exchange rate.

The statement made by the recently elected president of Nigeria served as a major catalyst for the spike in exchange rates and helped put this currency loss into perspective. He announced the removal of oil subsidies in his inaugural speech as president. This policy shift, intended to solve economic issues, had a noticeable and quick effect on the foreign exchange market. The plotted data makes it evident that the removal of oil subsidies was a major factor in the increase in EURO and RIYAL rates from June to December.

The justifications for the currency changes that have been found highlight how closely economic policies and exchange rate movements are related. Despite being aimed at addressing economic issues, the removal of oil subsidies clearly had a significant impact on the value of the Naira relative to other currencies. This analysis illustrates the complex relationship among economic factors that impact exchange rates and highlights the necessity of having an in-depth understanding of the policy consequences on currency values.

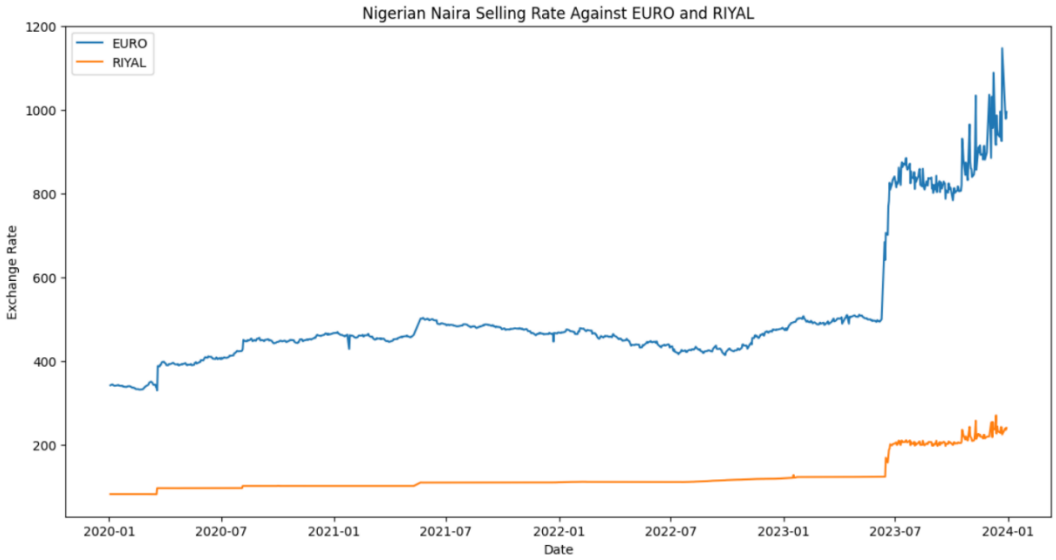

Figure 5: Plot of the daily Nigerian Naira to EURO and RIYAL exchange rates from January 2020 to December 2023.

The findings were instructive regarding the comparison of deep learning and machine learning models for predicting the exchange rates between the Nigerian Naira and the EURO and RIYAL. Each distribution's performance was assessed using the main evaluation metrics, such as RMSE and MAE, to give a thorough picture of the model's efficacy.

Table 11, presents the results of the competing models applied to the Naira against EURO exchange rate, revealing varying degrees of accuracy and performance. The XGBoost and Random Forest models exhibit similar levels of effectiveness, with RMSE and MAE values around 425, indicating reasonable predictive capabilities. LightGBM, while still competitive, shows a slightly higher error. In contrast to traditional machine learning models, the LSTM model stands out with significantly lower RMSE and MAE values of 5.47 and 4.58, respectively, indicating that the LSTM model excels in capturing the temporal patterns and dynamics of the EURO exchange rate. The LSTM's performance suggests that it may be well-suited for time series data with sequential dependencies.

A graphical depiction of the relative performance metrics for the different machine learning model algorithms is shown in Figure 6. Finding the best accuracy scores attained by various model algorithms is made easier with the help of the visual display.

Table 11: Comparative performance of machine learning and deep learning models for Nigerian Naira against EURO exchange rate.

Model	RMSE	MAE
XGBoost	425.3055	425.0334
Random Forest	424.6451	424.3535
LightGBM	428.1153	427.8973
LSTM	5.4722	4.5809

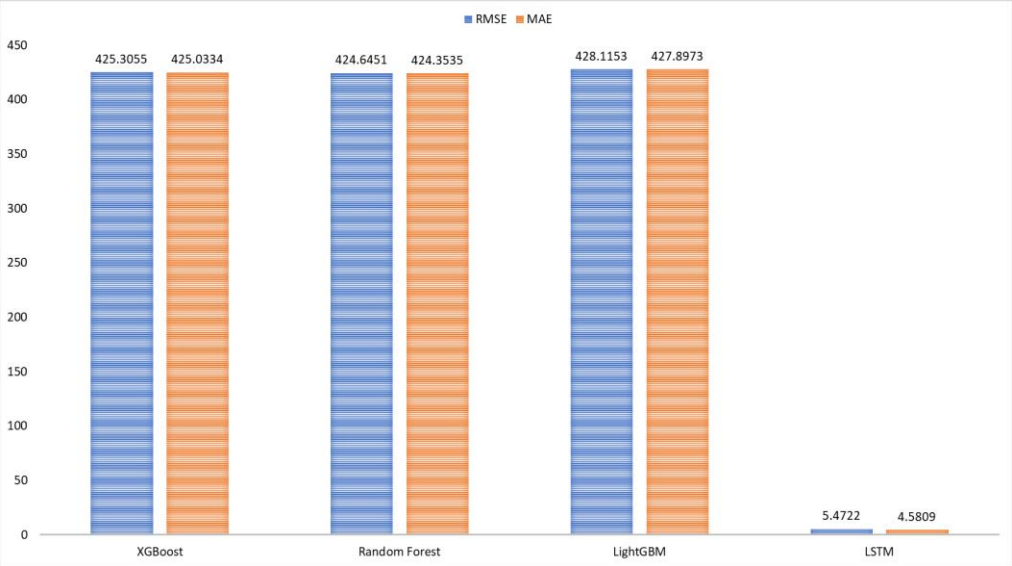

Figure 6: Comparative performance metrics across various competing algorithms against EURO exchange rate.

In Table 12, the evaluation results of machine learning models applied to the Naira against RIYAL exchange rate depict distinct performance characteristics. Both XGBoost and Random Forest models demonstrate comparable accuracy, with RMSE and MAE values around 103, indicating their effectiveness in predicting RIYAL exchange rates. The LightGBM model, while still providing reasonably accurate forecasts, exhibits slightly higher error metrics. In contrast, the LSTM model outperforms all other models significantly, indicating remarkable accuracy with minimal RMSE and MAE values of 1.08 and 0.93, respectively.

A graphical representation of the comparative performance measures amongst competing algorithms can be found in Figure 7. Finding the best accuracy ratings that various model algorithms have achieved is made easier with the help of this graphic depiction.

Table 12: Comparative performance of machine learning and deep learning models for Nigerian Naira against RIYAL exchange rate.

Model	RMSE	MAE
XGBoost	103.6061	103.5478
Random Forest	103.4412	103.3784
LightGBM	104.2547	104.2080
LSTM	1.0770	0.9347

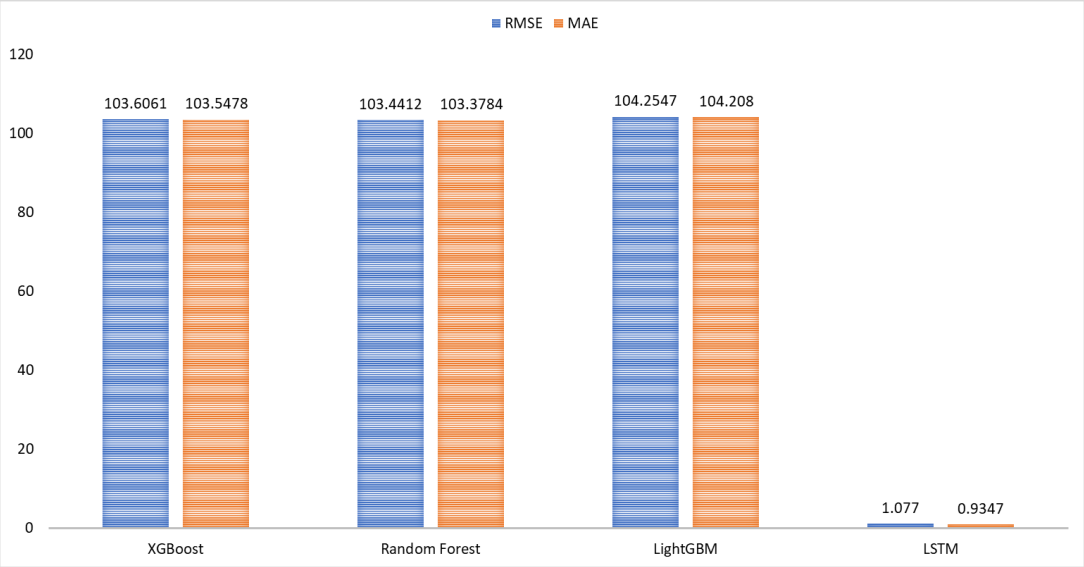

Figure 12: Comparative performance metrics across various competing algorithms for RIYAL exchange rate.

6. Conclusion

This research introduces the Topp-Leone Burr X distribution (TLBXD), a novel and versatile probability distribution derived from the Topp-Leone-G family. The TLBXD was specifically developed to address the challenges of modelling heterogeneous datasets that classical distributions struggle to accurately represent. Through comprehensive mathematical and statistical derivations, we established the properties of the TLBXD, making it a valuable tool for analyzing complex data structures. The application of the TLBXD to real-world datasets, specifically the exchange rates of the Nigerian Naira against the EURO and RIYAL, established the superior performance of the proposed distribution over existing sub-models. The TLBXD effectively captured the variations in these financial time series, underscoring its potential as a robust model for lifetime data analysis. In the prediction phase, we compared the forecasting abilities of ML and DL models, including XGBoost, Random Forest,

LightGBM, and LSTM. The LSTM model, a deep learning algorithm, consistently outperformed the machine learning models in terms of accuracy, as reflected by significantly lower RMSE and MAE values for both exchange rate datasets.

Funding: This study was financially supported by the Yayasan Universiti Teknologi PETRONAS: Fundamental Research Grant (YUTP-FRG) with the grant cost centre 015LC0-463.

Acknowledgements: The authors express their gratitude to Universiti Teknologi PETRONAS, Malaysia for their valuable support throughout the project.

REFERENCE

[1] A.A. Suleiman, H. Daud, M. Othman, A. Husin, A.I. Ishaq, R. Sokkalingam, I.K. Khan, Forecasting the Southeast Asian currencies against the British pound sterling using probability distributions, Data Sci. Insights 1 (2023), 31-51.

[2] A.I. Ishaq, A.A. Abiodun, A new generalization of dagum distribution with application to financial data sets, in: 2020 International Conference on Data Analytics for Business and Industry: Way Towards a Sustainable Economy (ICDABI), IEEE, Sakheer, Bahrain, 2020: pp. 1–6. https://doi.org/10.1109/ICDABI51230.2020.9325637.

[3] W.I. Burr, Cumulative frequency functions, Ann. Math. Stat. 13.2 (1942), 215-232. https://www.jstor.org/stable/2235756.

[4] A. Rabie, J. Li, E-Bayesian estimation for Burr-X distribution based on generalized type-I hybrid censoring scheme, Amer. J. Math. Manage. Sci. 39 (2020), 41–55. https://doi.org/10.1080/01966324.2019.1579123.

[5] A.A. Sanusi, S.I.S. Doguwa, I. Audu, Y.M. Baraya, Burr X exponential – G family of distributions: Properties and application, Asian J. Prob. Stat. 7 (2020), 58–75. https://doi.org/10.9734/ajpas/2020/v7i330186.

[6] A.K. Mahto, Y.M. Tripathi, S.J. Wu, Statistical inference based on progressively type-II censored data from the burr X distribution under progressive-stress accelerated life test, J. Stat. Comp. Simul. 91 (2021), 368–382. https://doi.org/10.1080/00949655.2020.1815021.

[7] K. Aidi, N.S. Butt, M.M. Ali, M. Ibrahim, H.M. Yousof, W.A.M. Shehata, A modified chi-square type test statistic for the double burr X model with applications to right censored medical and reliability data, Pak. J. Stat. Oper. Res. 17 (2021), 615–623. https://doi.org/10.18187/pjsor.v17i3.3888.

[8] R.A.R. Bantan, C. Chesneau, F. Jamal, I. Elbatal, M. Elgarhy, The truncated burr X-G family of distributions: Properties and applications to actuarial and financial data, Entropy 23 (2021), 1088. https://doi.org/10.3390/e23081088.

[9] H. Karamikabir, M. Afshari, M. Alizadeh, H.M. Yousof, The odd log-logistic burr-X family of distributions: Properties and applications, J. Stat. Theory Appl. 20 (2021), 228-241. https://doi.org/10.2991/jsta.d.210609.001.

[10] A. Algarni, A. M. Almarashi, I. Elbatal, A. S. Hassan, E.M. Almetwally, A. M. Daghistani, M. Elgarhy, Type I half logistic burr X-G family: Properties, bayesian, and non-bayesian estimation under censored samples and applications to COVID-19 data, Math. Probl. Eng. 2021 (2021), 5461130. https://doi.org/10.1155/2021/5461130.

[11] A.A. Al-Babtain, I. Elbatal, H. Al-Mofleh, A.M. Gemeay, A.Z. Afify, A.M. Sarg, The flexible burr X-G family: Properties, inference, and applications in engineering science, Symmetry 13 (2021), 474. https://doi.org/10.3390/sym13030474.

[12] F.G. Akgül, B. Şenoğlu, Inferences for stress–strength reliability of burr type X distributions based on ranked set sampling, Commun. Stat. – Simul. Comp. 51 (2022), 3324–3340. https://doi.org/10.1080/03610918.2020.1711949.

[13] R. Pakyari, A. Baklizi, On goodness-of-fit testing for burr type X distribution under progressively type-ii censoring, Comp. Stat. 37 (2022), 2249–2265. https://doi.org/10.1007/s00180-022-01197-5.

[14] O.H.M. Hassan, I. Elbatal, A.H. Al-Nefaie, M. Elgarhy, On the Kavya–Manoharan–Burr X model: Estimations under ranked set sampling and applications, J. Risk Financial Manage. 16 (2022), 19. https://doi.org/10.3390/jrfm16010019.

[15] B.P. Tlhaloganyang, W. Sengweni, B. Oluyede, The the gamma odd burr X-G family of distributions with applications, Pak. J. Stat. Oper. Res. (2022), 721–746. https://doi.org/10.18187/pjsor.v18i3.4045.

[16] A. Fayomi, A.S. Hassan, H. Baaqeel, E.M. Almetwally, Bayesian inference and data analysis of the unit–power burr x distribution, Axioms 12 (2023), 297. https://doi.org/10.3390/axioms12030297.

[17] C.W. Topp, F.C. Leone, A family of J-shaped frequency functions, J. Amer. Stat. Assoc. 50 (1955), 209–219. https://doi.org/10.1080/01621459.1955.10501259.

[18] A. Al-Shomrani, O. Arif, A. Shawky, S. Hanif, M.Q. Shahbaz, Topp–leone family of distributions: Some properties and application, Pak. J. Stat. Oper. Res. 12 (2016), 443. https://doi.org/10.18187/pjsor.v12i3.1458.

[19] M.N. Atchadé, M. N'bouké, A.M. Djibril, S. Shahzadi, E. Hussam, et al. A new power Topp–Leone distribution with applications to engineering and industry data, PLOS ONE 18 (2023), e0278225. https://doi.org/10.1371/journal.pone.0278225.

[20] M. Muhammad, L. Liu, B. Abba, I. Muhammad, M. Bouchane, H. Zhang, S. Musa, A new extension of the Topp–Leone-family of models with applications to real data, Ann. Data Sci. 10 (2023), 225–250. https://doi.org/10.1007/s40745-022-00456-y.

[21] S. Saini, S. Tomer, R. Garg, Inference of multicomponent stress-strength reliability following Topp-Leone distribution using progressively censored data, J. Appl. Stat. 50 (2023), 1538–1567. https://doi.org/10.1080/02664763.2022.2032621.

[22] R.A.H. Mohamed, M. Elgarhy, M.H. Alabdulhadi, E.M. Almetwally, T. Radwan, Statistical inference of truncated cauchy power-inverted Topp–Leone distribution under hybrid censored scheme with applications, Axioms 12 (2023), 148. https://doi.org/10.3390/axioms12020148.

[23] M. Gabanakgosi, B. Oluyede, The Topp-Leone type II exponentiated half logistic-g family of distributions with applications, Int. J. Math. Oper. Res. 25 (2023), 85–117. https://doi.org/10.1504/IJMOR.2023.131382.

[24] J.C. Ehiwario, J.N. Igabari, P.E. Ezimadu, The alpha power Topp-Leone distribution: properties, simulations and applications, J. Appl. Math. Phys. 11 (2023), 316–331. https://doi.org/10.4236/jamp.2023.111018.

[25] B. Oluyede, T. Moakofi, The Gamma-Topp-Leone-type II-exponentiated half logistic-G family of distributions with applications, Stats 6 (2023), 706–733. https://doi.org/10.3390/stats6020045.

[26] A.S. Mohammed, F.I. Ugwuowo, On transmuted exponential-Topp Leon distribution with monotonic and non-monotonic hazard rates and its applications, 16 (2021), 197-209. https://doi.org/10.24412/1932-2321-2021-465-197-209.